Current Applied Science and Technology Vol. 23 No. 4 (July-August 2023)

Research article

New Azo-Schiff Compounds and Metal Complexes Derived from 2-Naphthol Synthesis, Characterization, Spectrophotometric, and Study of Biological Activity

Hawraa Mahdi Alabidi[1], Ali Mahdi Farhan[2], Nuha Salman Salh[1] and Ahmed Abduljabbar Jaloob Aljanaby[3]*

[1]*Department of Chemistry, Faculty of Science, University of Kufa, Kufa, Iraq*
[2]*Ministry of Education, Al-Najaf, Iraq*
[3]*Department of Biology, Faculty of Science, University of Kufa, Kufa, Iraq*

Received: 6 July 2022, Revised: 23 August 2022, Accepted: 20 December 2022

DOI: 10.55003/cast.2022.04.23.007

Keywords

azo;
schiff base;
spectrophotometric studies;
ıonization constant;
complexes;
antibacterial evaluation

Abstract

This research involved synthesizing two compounds as derivatives of 2-naphthol by the classical method. The azo coupling compound was prepared via diazonium salt of 4-amino acetophenone followed by 2-naphthole. The azo-Schiff molecule was synthesized through condensation of an azo compound with 5-amino salicylic acid in an acidic medium. Using spectrum approaches, the new compounds are characterized (^{13}C-NMR, ^{1}H-NMR, FT-IR). The acid-base characteristics were investigated at various pH levels (0.67-12), and the ionization and protonation constants were determined. Spectroscopic methods were used to identify new copper (II), nickel (II), and cobalt (II) complexes of the azo-Schiff base ligand. All the compounds were evaluated for antibacterial activity against bacteria such as *Staphylococcus aureus* (Gram-positive bacteria) and *Escherichia coli* (Gram-negative bacteria). It was found that the coordination complexes of Cu and Co had an antibacterial effect on both concentrations against *Staphylococcus aureus.*

1. Introduction

Azo compounds are one of the most widely used chemical groups of organic compounds, with various applications [1] in advanced organic synthesis to high technology areas such as liquid crystalline displays, ink-jet printers, lasers, and electro optical devices [2]. They are also known to have wide ranges of biological effects such as DNA, RNA inhibition and protein synthesis, carcinogenesis, and nitrogen fixation [3].

*Corresponding author: E-mail: aliphd256@gmail.com

Since azo compounds can form organometallic compounds with transition metal ions, there have been the focus of numerous spectroscopic studies to identify or elucidate structures [4]. Schiff bases are chemical compounds synthesized by condensation of a ketone or aldehyde with a substituted primary amine [5-7], and they were reported by Hugo Schiff in 1864 [8]. Also, Schiff bases are known as the azomethine compounds [9]. The existence of a lone pair of electrons in the azomethine group's sp2 hybridized nitrogen atom orbital is of major chemical and biological significance, according to various studies [10]. Thus, both the azo and Schiff base compounds are known to be antifungal, anti-bacterial [11-14], anti-inflammatory and anti-cancer [15, 16]. In recent years, azo and Schiff base compounds have drawn the attention of researchers to their development and study of application in a variety of fields. For example, Al Zoubi *et al*. [17] prepared new complexes from azo-Schiff base ligand which derived from 4-aminoantypyrine and evaluated as antibacterial activity. Moreover, Alabidi *et al*. [18] developed a new azo molecule obtained from 2-naphthol, which was used to evaluate Zn(II) in pharmaceutical formulations using spectrophotometry. Consequently, this research involved the preparation of azo-Schiff base compounds and their chelate complexes and the study of their biological activities which could be used for the manufacturing of an ointment in order to treat inflammation of wounds and burns caused by pathogenic bacteria.

2. Materials and Methods

The NMR spectra were recorded on a Bruker-NMR 400 MHZ using the solvent DMSO–d^6. The FT-IR spectra were obtained using a Shimadzu spectrophotometer and a KBr disk. A double beam Shimadzu 1700 UV spectrometer was used to record the UV spectra. TLC was used to check the reaction bath, which was then visualized in iodine vapor. In open capillary tubes, melting points were determined.

2.1 Chemical synthesis

2.1.1 Synthesis of azo compound

According to Alabidi *et al*. [19], azo compound (L1) was prepared by dissolving the 4-Amino acetophenone (375 mg, 2.77 mmol) in 20 ml of absolute ethanol and then added to 2 ml of HCl (conc.). Then, stirred for 20 min in an ice bath; after that, an ice-cold solution of sodium nitrite $NaNO_2$ (10 %) 25 ml was added drop by drop on a period of 35 min. The solution became brown, and was added dropwise to another ice-cold solution of 2- naphthol (400, 2.77 mmol) in 20 ml alkaline ethanol, and constantly stirred at 50^{o}C overnight. Diluted ammonia and hydrochloric acid were used to neutralize the reaction mixture until pH= 7. Afterwards, the resulting product was filtered before being washed in cold distilled water and dried.

Yield: 600 mg 74 %, m.p:141-143 FT-IR (KBr) (cm^{-1}): 3330 (OH), 2931 and 2882 (C-H,aliph), 1652 (C=O, Keto), 1598 (C=C, arom), 1396 (N=N).^{1}H-NMR, 8.49-8.51 (d,2H , H13+15), 8.23-8.25 (d ,2H, H12+16) , 8.14-8.11 (d,1H, H-4), 8.01-7.98 (d, 1H, H-9, 7.92-7.94 (d, 1H, H-6), 7.78-7.80 (d ,1H , H-3), 7.64-7.66 (t, 1H , H-8), 8.53-8.55 (t ,1H, H-7), 6.83 (s, 1H, OH-arom), 2.41 (s, 3H, Me-Keto). ^{13}C-NMR (100 MHz, DMSO-d6) 196.6 (Keto C-18), 142.5 (C-11), 134.0 (C-14), 132.7 (C-2), 130.1(C-5), 129.6 (C-4), 129.2 (C-10), 128.9 (C-1), 128.1 (C-8), 126.9 (C-7), 125.7 (C-6+9), 122.9 (C-3), 121.8 (C-13+15), 117.1 (C-12+16), 26.6 (Me-18)

2.1.2 Synthesis of azo-Schiff compound (L_2) [20, 21]

A solution consisting of L1 (350 mg, 1.206 mmol) in 30 ml of ethyl alcohol was added to another solution (185 mg, 1.206 mmol) of 5-amino salicylic acid, with a drop of acetic acid, and the resultant mixture was heated in reflux for 8-10 h. With chloroform-methanol (4:1) as eluents, the progress of the reaction was observed using TLC. The solid product was collected, filtered, collected, and recrystallized from ethanol to yield the desired product after cooling.

Yield: 550 mg 81 %, yellow powder, m.p:192-194 R*f* = 0.35 FT-IR (KBr) (cm^{-1}): 3425 (OH), 2927 and 2783 (C-H aliph), 1660 (C=O, Carboxylic), 1645 (C=N), 1598 (C=C, arom), 1452 (N=N). ^{1}H-NMR, 15.88 (br,1H, COOH), 8.42-8.44 (d ,2H , H13+15), 8.17-8.19 (d, 2H, H12+16), 8.05-8.07 (d, 1H, H-4), 7.92-7.94 (d, 1H, H-20), 7.87-7.87 (d, 1H, H-3), 6.73 (s, 1H, OH, C22-arom), 7.58-7.60 (t, 1H, H-8), 7.47-7.49 (t, 1H, H-7), 7.18 (s, 1H, H-24), 6.87-6.89 (d, 1H, H-6), 6.75-6.77 (d, 1H, H-6), 6.67-6.69 (d, 1H, H-21), 6.55 (s, 1H, OH-arom), 2.38 (s, 3H, Me-Keto). ^{13}C-NMR (100 MHz, DMSO-d6) 171.6 (COOH), 154.6 (C=N, C-17), 146.5 (C-23), 142.4 (C-22+11), 138.7 (C-19), 134.0 (C-10), 132.6 (C-2) , 131.5 (C-14), 130.5 (C-21), 130.2 (C-5), 129.6 (C-20+4), 129.2 (C-10), 128.9 (C-1), 128.1 (C-8), 126.9 (C-7), 125.7 (C6+9), 123.4 (C13+15), 122.9 (C-3), 121.8 (C12+16), 26.6 (Me-18).

2.1.3 Synthesis of metal complexes [22]

The metal complexes were obtained by adding 2 mmol of azo-Schiff ligand in 30 ml ethyl alcohol and added it to metal salts drop by drop of cobalt(II), nickel(II), and copper(II) by a stoichiometric amount of (2:1) (ligand: metal). The solution was added to 25 ml of distilled water. Under reflux, the resultant mixture was stirred for 2 h. The products of complexes were collected, washed, purified, and left overnight at 50ºC for dryness. The general equation of synthesized metal complexes is shown below.

$$MCl_2 + 2HL \rightarrow [M\,L_2\,(\,H_2O\,)_2] + 2HCl$$

Cu^{+2} complex: FT-IR (KBr) (cm-1): 3446 (OH), 2926 and 2852 (C-H, aliph), 1681 (C=O, carboxylic), 1639 (C=N), 1558 (C=C, arom), 1413 (N=N).
Ni^{+2} complex: FT-IR (KBr) (cm-1): 3448 (OH), 2924 and 2852 (C-H, aliph), 1678 (C=O, carboxylic), 1595 (C=N), 1498 (C=C, arom), 1440 (N=N).
Co^{+2} complex: FT-IR (KBr) (cm-1): 3446 (OH), 2931 (C-H, aliph), 1680 (C=O, carboxylic), 1579 (C=N), 1508 (C=C, arom), 1417 (N=N).

2.2. Prepared acid-base solutions [23]

To evaluate the protonation and ionization constants, as well as the effect of pH on the absorption spectra of azo-Schiff compound, multiple pH values of buffer solutions (acetate and universal) were prepared (1 < -12), and concentrations of ligand are ($1x10^{-3}$) M. The absorbance of these solutions was measured at the wavelength of 300-450 nm as a blank of buffer solution. The constants were determined using the half-length approach.

2.3. Antibacterial activity test

Agar well diffusion has demonstrated the antibacterial activity of ligand, Co, Ni, and Cu complexes [24]. Fifty mg/ml and 200 mg/ml were made from each compound [25]. Two multi-drug resistance pathogenic bacteria were selected: *Staphylococcus aureus* (Gram-positive bacteria) and *Escherichia*

coli (Gram-negative bacteria) were provided from the Department of Microbiology, Faculty of Science, University of Kufa. Three wells made in Muller-Hinton agar surface by cock borer (10 mm) swabbed with two pathogenic bacteria according to 0.5 McFarland turbidity [26]. Each well received 40 µL of any dilution, which was incubated at 37°C for 24 h after being left at 20°C for two h. In all tests, the diameter of the inhibition zone was measured in mm done in three replicates [27, 28]. According to SPSS V.10 windows software, a P-value greater than or equal to 0.05 was considered to be significant when compared to the diameters of inhibition zones [29, 30].

3. Results and Discussion

3.1 Chemistry synthesis

To synthesize the azo compound, firstly prepared diazonium salt of 4-aminoacetophenone and coupled it with 2-naphthol stirred in an alkaline solution according to Figure 1.

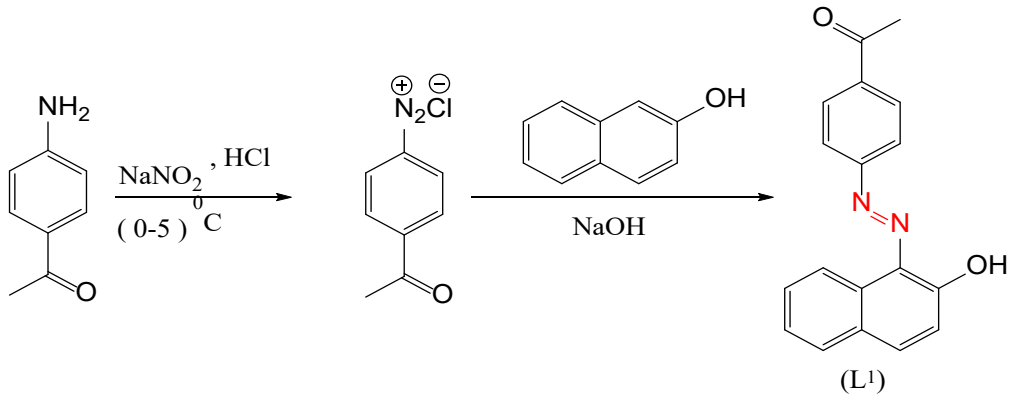

Figure 1. Synthesis of azo compound

The chemical structure was elucidated by spectral methods. The number of signals in the ^{1}H-NMR spectra of azo compound (L1) was observed due to the 10 protons back to the three aromatic rings were observed in the δ ~7.53-8.51 ppm range. Some of these doublet signals appeared at chemical shift (δ ~8.49-8.51ppm) for H_{13+15} due to the withdrawing induced by the keto group. The other triplet signals appeared at the field (δ ~8.01-7.98, 7.92-7.94 and 7.78-7.80 ppm) due to protons H_9, H_6, and H_3, respectively while the singlet signal of hydroxyl group showed at (d ~6.83 ppm). At a lower field, Me-keto appeared at (d ~ 2.41 ppm), as shown in Figures 2 and 3.

In the ^{13}C-NMR spectra, the signal of the carbonyl keto (C_{-17}) appeared at 196 ppm, while the signals back to 16 aromatic carbon atoms were observed at a range of 117-142 ppm. At this time, the signal of the methyl group was shown at 26 ppm (Figures 4 and 5).

Azo-Schiff compound (L_2) was prepared via condensation of 5-aminosalsylic acid with azo derivative (L1) in an acidic solution, according to Figure 6.

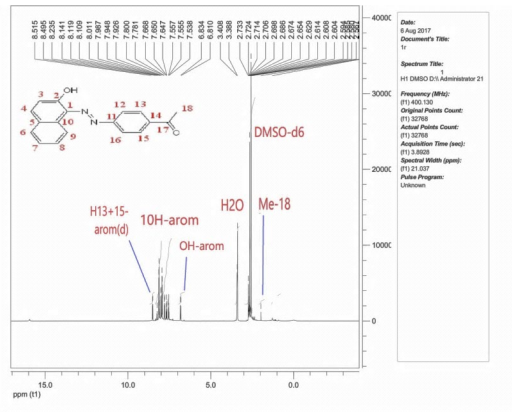

Figure 2. Azo compound (L_1), ^{1}H-NMR spectra

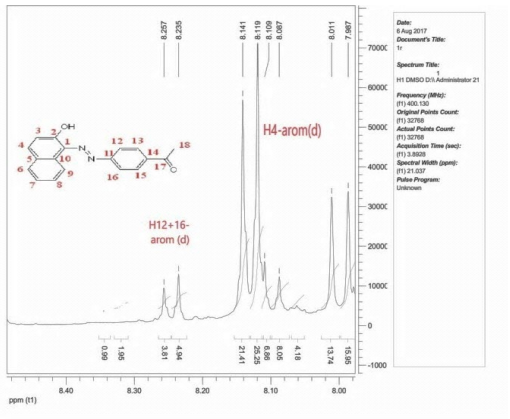

Figure 3. Azo compound (L_1), expansion ^{1}H-NMR spectra

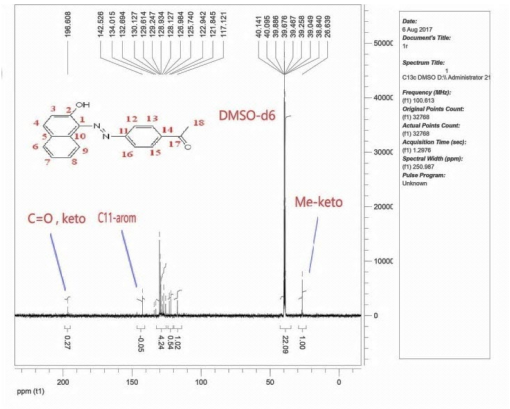

Figure 4. Azo compound, ^{13}C-NMR spectra

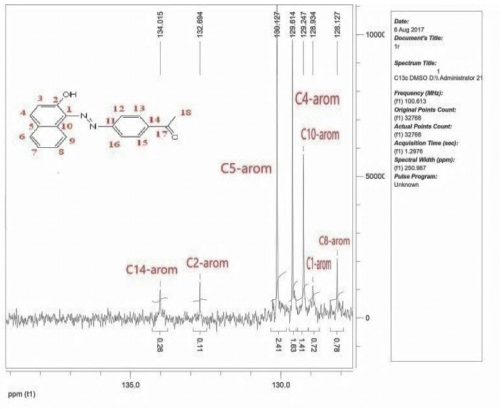

Figure 5. Azo compound, expansion ^{13}C-NMR spectra

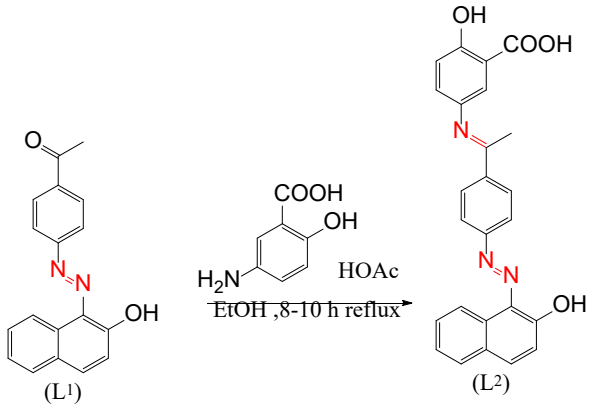

Figure 6. Synthesis of azo- Schiff compound

^{1}H- NMR spectra showed a new broad signal at the downfield (δ ~ 15.88 ppm) back to the proton of the carboxyl group; the bands of $H_{13,15}$ and $H_{12,16}$ appeared at a field less than the field of derivative (L1) at shift (δ ~8.42-8.44, and 8.17-8.19 ppm), respectively. Because of a change in the neighboring group from C=O to C=N, the new other singlet group appeared at the field (δ ~ 7.18 ppm) due to H_{-24} of benzoic acid derivative, as shown in Figures 7 and 8.

The ^{13}C-NMR spectra showed new signals at the downfield of the spectrum at shifts 171and 154 ppm due to the carboxyl (C_{-25}) and azomethane (C_{-17}) groups, respectively. Meanwhile, the signals at the range of δ ~115-146 ppm assigned to 22 carbon atoms of four aromatic rings, also the signal of methyl group was showed at δ ~26 ppm, as seen in Figures 9 and 10.

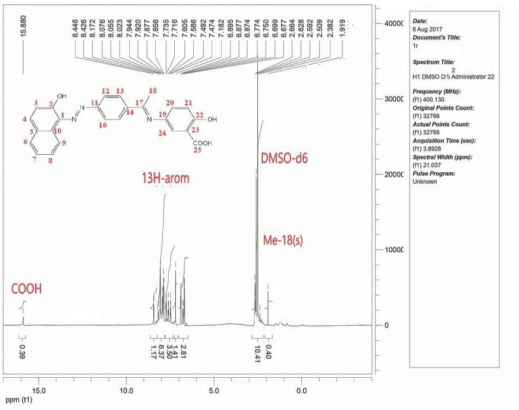

Figure 7. Azo-Schiff compound, ^{1}H-NMR spectra

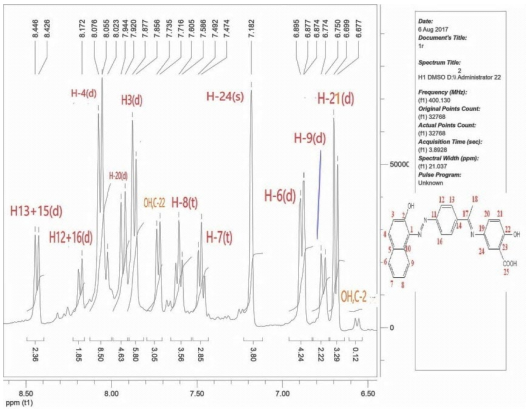

Figure 8. Azo-Schiff compound, expansion ^{1}H-NMR spectra

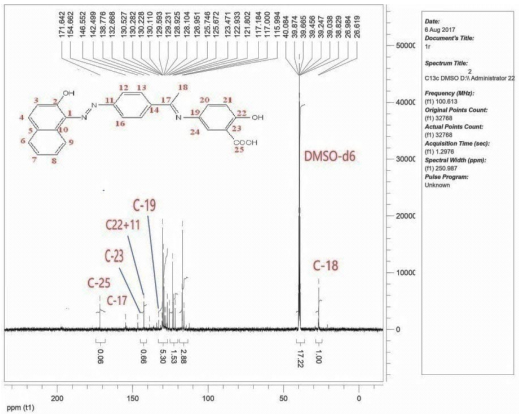

Figure 9. Azo-Schiff compound, ^{13}C-NMR spectra

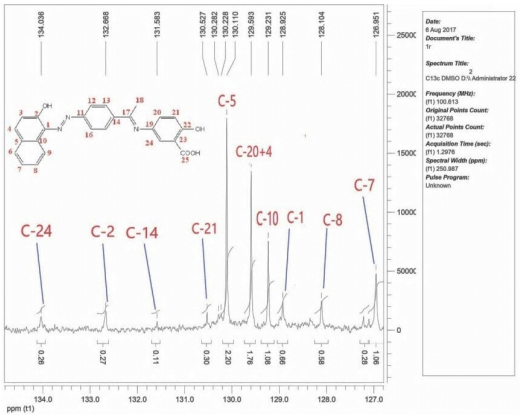

Figure 10. Azo-Schiff compound, expansion ^{13}C-NMR spectra

3.2 FT-IR Spectra

FT-IR of complexes (Figures 11-13) appeared very different from the ligand shown in Figure 14. The peak of hydroxyl and carbonyl groups shifted to the higher wave number, which can be due to

hydrogen bonding [31]. The wave number of azo groups shifted to the lower as a result of the coordinate. Therefore, the chemical structure of complexes can be found in Figure 15 via ligand: metals (2:1), so the hybridization of complexes is sp^3d^2, and the shape is octahedral [32].

3.3 Absorption spectra of azo-Schiff compound

The electronic absorption of ligand clearly shows three bands (Figure16) at different wavelengths. The n- π* transition was assigned to the first and second bands, which appeared at 206 and 320 nm, respectively. The other band observed at 486 nm, assigned π-π* transition, represents the λ_{max} of ligand [33]. This band displayed a red shift during metal ions coordination, as shown in Figures17-19.

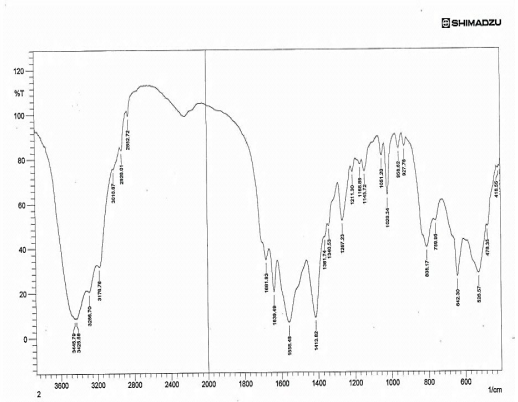

Figure 11. FT-IR of Co(II) complex

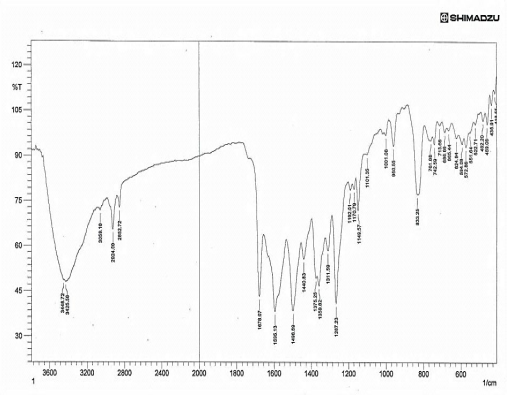

Figure 12. FT-IR of Ni(II) complex

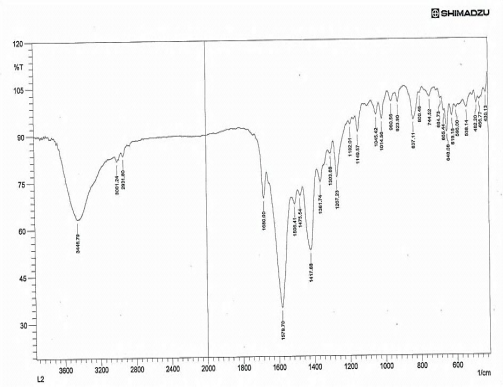

Figure 13. FT-IR of Cu(II) complex

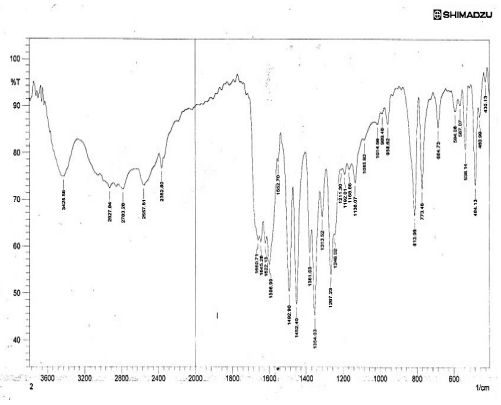

Figure 14. FT-IR of azo- Schiff compound

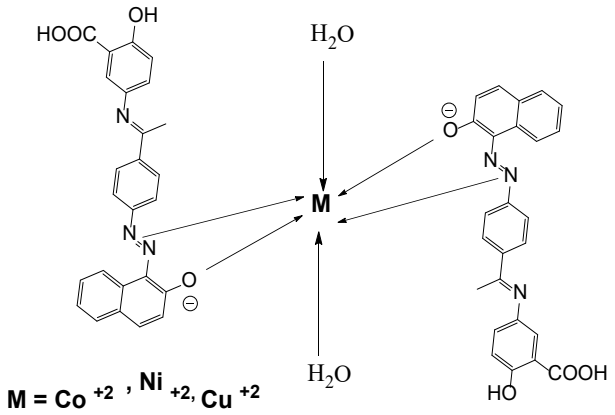

Figure 15. Chemical structure of complexes

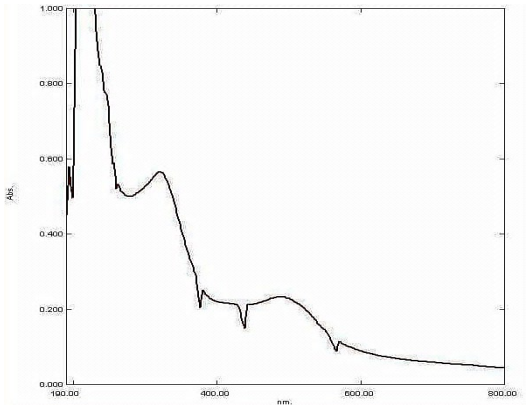

Figure 16. Absorption spectra of azo-Schiff

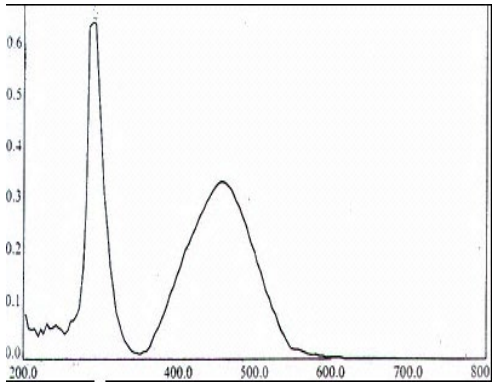

Figure 17. Absorption spectra of Co(II)

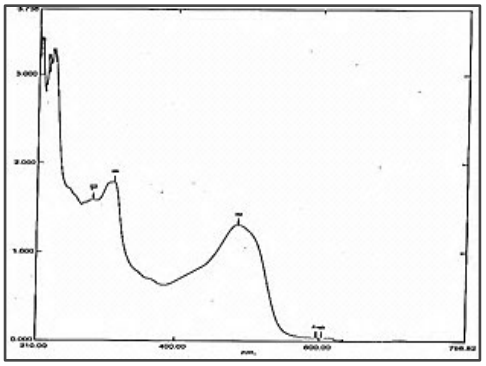

Figure 18. Absorption spectra of Cu(II) complex

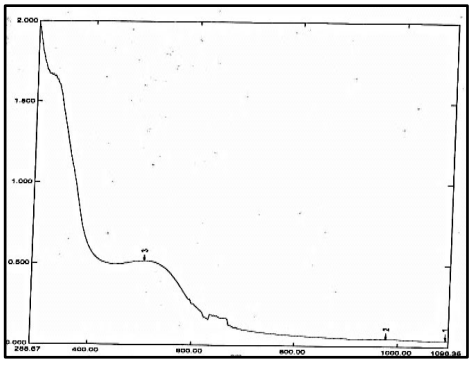

Figure 19. Absorption spectra of Ni(II) complex

3.4 Absorption spectra of azo-Schiff ligand in buffer solution

A series of buffer solutions were prepared at various pH to study the effect of pH on the azo-Schiff compound. The absorbance of concentration with the ligand is (1 x 10^{-3}–2x10^{-3}) at the wavelength of 300-450 nm, which represents graphically in Figure 20. The carboxyl group appeared at pH 7-8, while the hydroxyl group of naphthol appeared at pH 8-9. However, the hydroxyl group of benzoic acid derivative appeared at pH 10-11. In addition, the protonated forms appear at low pH values (1-4) (Figure 21). The results shown in Table 1 suggested the effect of pH on the azo-Schiff compound as shown in Figure 22.

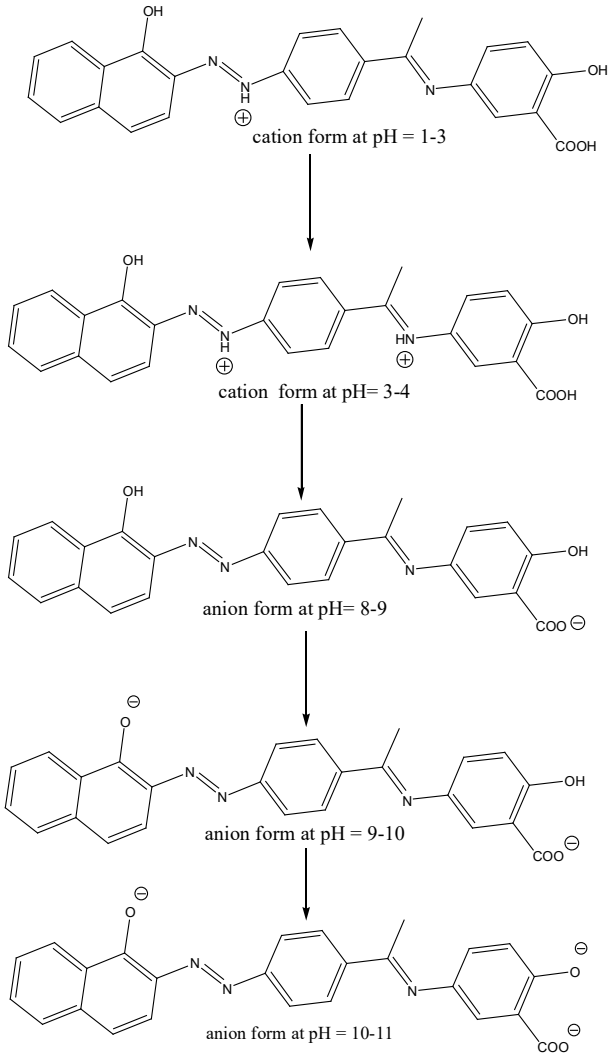

Figure 20. Acid-base properties of azo- Schiff compound

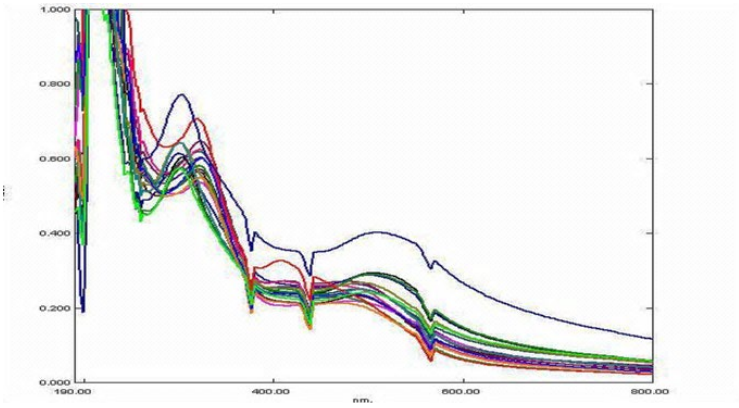

Figure 21. Absorption spectra of azo-Schiff compound at varying pH values

Table 1. The protonation (pk_p) and ionization (pk_a) constants of the Azo-Schiff compound

Compound	λ(*nm*)	$A_{1/2}$	PK_{p1}	$A_{1/2}$	PK_{p2}	$A_{1/2}$	PK_{a1}	$A_{1/2}$	PK_{a2}	$A_{1/2}$	PK_{a3}
Azo-Schiff	320	0.674	1.2	0.608	4.4	0.584	7.4	0.61	8.8	0.643	10.7

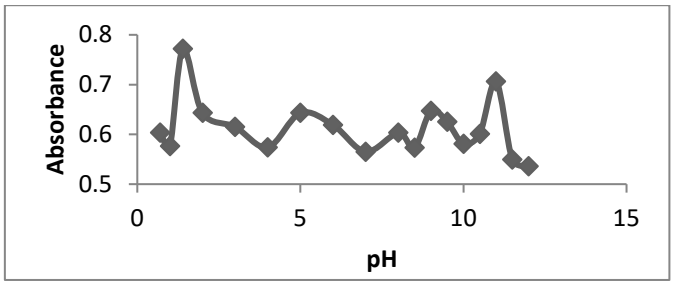

Figure 22. Absorbance-pH curves of azo-Schiff compound

The protonation and ionization constants [23] were estimated using the half-height approach to determine pka values from the built absorbance–pH curves in Figure 22. The relationship: pK_a = pH at ($A_{1/2}$) when ($A_{1/2}$) = (A_l+A_{min})/2. Al means limited absorbance, and Amin means minimum absorbance.

3.5 Antibacterial activity

Our findings demonstrated that all derivative compounds have no antibacterial effect on *Escherichia coli*. While only Cu and Co have an antibacterial effect against *Staphylococcus aureus* at both concentrations (Figures 23 and 24). According to statistical analysis, the results indicate that the diameter of inhibition zones of Cu 50 mg/ml (12.967±0.29) and 100 mg/ml (13.267±0.39) had no statistically significant differences (P-value 0.2863) against *S. aureus* (Figure 25). In addition, there was no significant difference (P-value 0.1336) between the diameter of inhibition zones of Co 50 mg/ml (10.83±0.33) and 100 mg/ml (11.60±0.49) against *S. aureus* Figure 26. On the other hand, a significant increase (P-value 0.0042**) has been indicated between the diameter of inhibition zones in Cu 50 mg/ml as compared with Co 50 mg/ml against *S. aureus* (Figure 27). In addition,

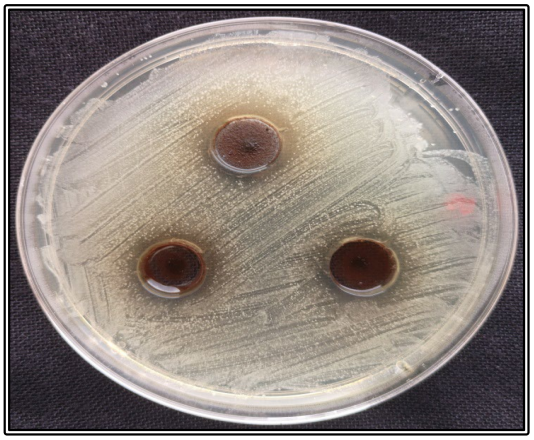

Figure 23. Antibacterial activity of Cu 100 mg/ml against *S. aureus*

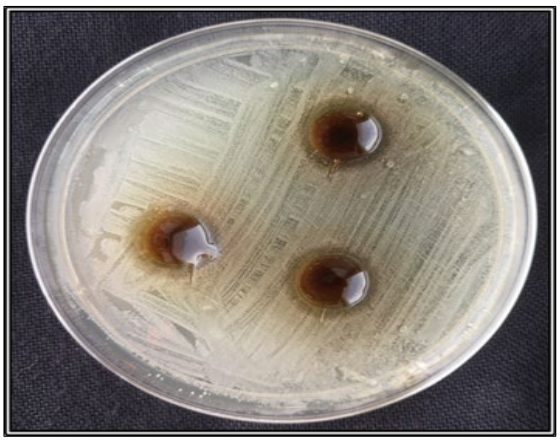

Figure 24. Diameters of inhibition zones of Co against *S. aureus*

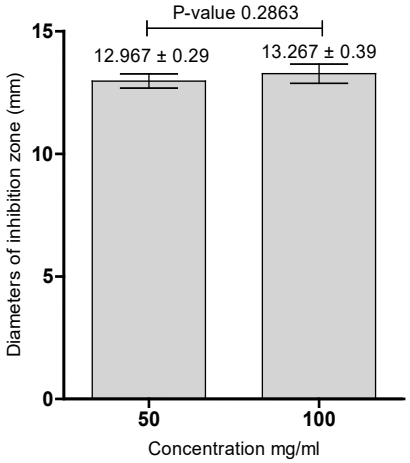

Figure 25. Diameters of inhibition zones of Cu against *S. aureus*

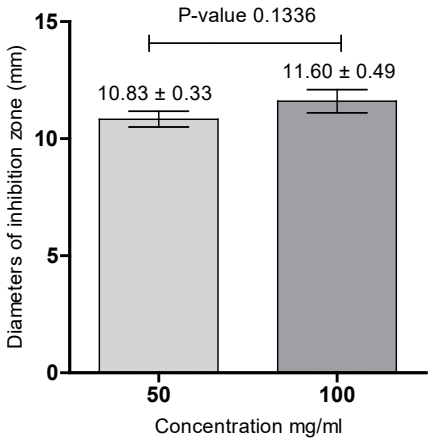

Figure 26. Diameters of inhibition zones of Co against *S. aureus*

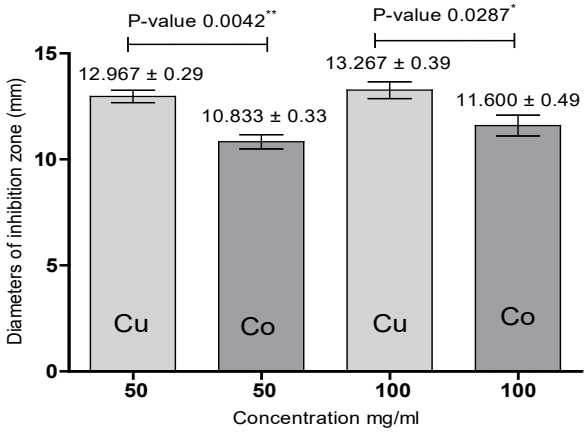

Figure 27. Comparison between diameters of inhibition zones of Cu and Co against *S. aureus*

when Cu 100 mg/ml was compared to Co 100 mg/ml against *S. aureus*, a significant increase (P-value 0.0287*) in the diameter of inhibitory zones was observed.

4. Conclusions

Three main complexes were synthesized in high yields, and the products were analyzed using several spectrum methods. Based on UV-Vis, FTIR, ^{1}HNMR, and ^{13}CNMR spectroscopy, a structure for complexes was proposed, showing that the N and O atoms in the azo-Schiff ligand bonded with metal ions. The (L_2) and its complexes were studied for antibacterial activity against *E. coli* and *S. aureus*. The antimicrobial screening revealed that none of the three complexes have the antibacterial activity against *E. coli* whereas Cu(II) and Co(II) complexes have the antibacterial activity against *S. aureus.*

5. Acknowledgements

Our thanks to Dr. Lamia A. Rusin for providing information about special part in analytical chemistry.

References

[1] Rezaei-Seresht, E., Mireskandari, E., Kheirabadi, M., Cheshomi, H., Rezaei-Seresht, H. and Aldaghi, L.S., 2017. Synthesis and anticancer activity of new azo compounds containing extended π-conjugated systems. *Chemical Papers*, 71(8), 1463-1469.

[2] El-Bindary, A.A., Hussein, M.A. and El-Boz, R.A., 2015. Molecular docking, theoretical calculations and potentiometric studies of some azo phenols. *Journal of Molecular Liquids*, 211, 256-267.

[3] Jarad, A.J., 2012. Synthesis and characterization of new azo dye complexes with selected metal ions. *Al-Nahrain Journal of Science*, 15(4), 74-81.

[4] Mahmoud, W.H., Omar, M.M. and Sayed, F.N., 2016., Synthesis, spectral characterization, thermal, anticancer and antimicrobial studies of bi dentate azo dye metal complexes. *Journal of Thermal Analysis and Calorimetry*, 124(2), 1071-1089.

[5] Al-Shareef, H.F., Elhady, H.A., Aboellil, A.H. and Hussein, E.M., 2016. Ammonium chloride catalyzed synthesis of novel Schiff bases from spiro [indoline-3, 4′-pyran]-3′-carbonitriles and evaluation of their antimicrobial and anti-breast cancer activities. *Springer Plus*, 5(1), DOI: 10.1186/s40064-016-2458-0.

[6] Sahan, F., Kose, M., Hepokur, C., Karakas, D. and Kurtoglu, M., 2019. New azo-azomethine-based transition metal complexes: Synthesis, spectroscopy, solid-state structure, density functional theory calculations and anticancer studies. *Applied Organometallic Chemistry*, 33(7), DOI: 10.1002/aoc.4954.

[7] Bhowmick, A., Islam, M., Bhowmick, R., Sarkar, M., Shibly, A. and Hossain, E., 2019. Synthesis and structure determination of some Schiff base metal complexes with investigating antibacterial activity. *American Journal of Chemistry*, 9(1), 21-25.

[8] de Fátima, Â., Pereira, C., Olímpio, C.R.S.D.G., Oliveira, B.G.D.F., Franco, L.L. and da Silva, P.H.C., 2018. Schiff bases and their metal complexes as urease inhibitors–a brief review. *Journal of Advanced Research*, 13, 113-126.

[9] Kribaa, L., Atia, S., Boudehane, A., Bader, R.M.M. and Gherraf, N., 2019. Synthesis, characterization and antioxidant activity studies of new Azo-compounds. *Journal of Biochemical Technology*, 10(1), 85-90.

[10] Ashraf, M.A., Mahmood, K., Wajid, A., Maah, M.J. and Yusoff, I., 2011. Synthesis, characterization and biological activity of Schiff bases. *International Proceedings of Chemical, Biological and Environmental Engineering*, 10, 1-7.

[11] Eissa, H.H., 2013. Synthesis and characterization of new azo-Schiff bases and study biological activity. *Journal of Current Research in Science*, 1(2), 96-103.

[12] Erturk, A.G., 2020. Synthesis, structural identifications of bioactive two novel Schiff bases. *Journal of Molecular Structure*, 1202, DOI: 10.1016/j.molstruc.2019.127299.

[13] Salman, S.D. and Adnan, S., 2018. Synthesis, characterization of some new derivatives of (oxazpine, thiazinone and hydroquinazoline)-azo group from amine compounds. *Eurasian Chemico-Technological Journal*, 20(3), 264-276.

[14] Abd-Elzaher, M.M., Labib, A.A., Mousa, H.A., Moustafa, S.A., Ali, M.M. and El-Rashedy, A.A., 2016. Synthesis, anticancer activity and molecular docking study of Schiff base complexes containing thiazole moiety. *Beni-Suef University Journal of Basic and Applied Sciences*, 5(1), 85-96.

[15] Ghasemi, Z., Azizi, S., Salehi, R. and Kafil, H.S., 2018. Synthesis of azo dyes possessing N-heterocycles and evaluation of their anticancer and antibacterial properties. *Monatshefte für Chemie-Chemical Monthly*, 149(1), 149-157.

[16] Sarangi, P.K.N., Sahoo, J., Behera, S., Paidesetty, S.K. and Mohanta, G.P., 2017. Cytotoxic investigation of some newly synthesized quinoline-thiazole based azo compounds. *Indian Journal of Chemistry*, 56, 1256-1264.

[17] Al Zoubi, W., Al-Hamdani, A.A.S. Ahmed, S.D. and Ko, Y.G., 2018. A new azo-Schiff base: Synthesis, characterization, biological activity and theoretical studies of its complexes. *Applied Organometallic Chemistry*, 32(1), DOI: 10.1002/aoc.3895.

[18] Alabidi, H.M., Farhan, A.M., and Al-Rufaie, M.M., 2021. Spectrophotometric determination of Zn (II) in pharmaceutical formulation using a new Azo reagent as derivative of 2-naphthol. *Current Applied Science and Technology*, 21(1), 176-187.

[19] Alabidi, H.M., Alabidi, A.M. and Makki, N.F., 2018. Synthesis and spectroscopic studying of new Azo Ligand from 2-Naphthol derivative and it's complexes with some transition metal ions. *Al-Qadisiyah Journal of Pure Science*, 23(1), 186-195.

[20] Abdul-Rida, N.A., Farhan, A.M., Al-Masoudi, N.A., Saeed, B.A., Miller, D. and Lin, M.F., 2020. A novel pregnene analogs: synthesis, cytotoxicity on prostate cancer of PC-3 and LNCPa-AI cells and in silico molecular docking study. *Molecular Diversity*, 25(2), 661-671.

[21] AL-Rida, N.A.A. and Farhan, A.M., 2019. Synthesis, characterization and study biological activity of some new derivatives of steroid analogs. *Journal of Physics: Conference Series*, 1294(5), DOI: 10.1088/1742-6596/1294/5/052002.

[22] Alabidi, H., Farhan, A., Al-labban, H. and Aljanaby, A., 2022. New derivatives from 4-amino anti-pyrine and vanillin, synthesis characterization and antibacterial activity. *Egyptian Journal of Chemistry*, 65(10), DOI: 10.21608/ejchem.2022.135727.5977.

[23] Asaad, A.A. and Rusin, L.A., 2016. Synthesis and spectrophotometric study of some new azo dyes derived from procaine. *Asian Journal of Research in Chemistry and Pharmaceutical Sciences*, 4(1), 11-20.

[24] Aljanaby, A.A.J., 2018. Antibacterial activity of an aqueous extracts of *Alkanna tinctoria* roots against drug resistant aerobic pathogenic bacteria isolated from patients with burns infections. *Russian Open Medical Journal*, 7(1), DOI: 10.15275/rusomj.2018.0104.

[25] Adam, R.W., Al-Labban, H.M.Y., Aljanaby, A.A.J. and Abbas, N.A., 2019. Synthesis, characterization and antibacterial activity of some novel 1, 2, 3-triazol-chalcone derivatives from N-Acetyl-5H-dibenzo [b, f] azepine-5-carboxamide. *Nano Biomedicine and Engineering,* 11(2), 99-110.

[26] Yuan, G., Guan, Y., Yi, H., Lai, S., Sun, Y. and Cao, S., 2021. Antibacterial activity and mechanism of plant flavonoids to gram-positive bacteria predicted from their lipophilicities. *Scientific Reports*, 11(1), DOI: 10.1038/s41598-021-90035-7.

[27] Al-Labban, H.M.Y., Sadiq, H.M. and Aljanaby, A.A.J., 2019. Synthesis, characterization and study biological activity of some Schiff bases derivatives from 4-amino antipyrine as a starting material. *Journal of Physics: Conference Series*, 1294(5), DOI: 10.1088/1742-6596/1294/5/052007.

[28] Aljanaby, A.A.J. and Aljanaby, I.A.J., 2018. Prevalence of aerobic pathogenic bacteria isolated from patients with burn infection and their antimicrobial susceptibility patterns in Al-Najaf City, Iraq-a three-year cross-sectional study. *F1000 Research*, 7(1157), DOI: 10.12688/f1000research.15088.1.

[29] Hasan, T.H., Alasedi, K.K., Aljanaby, A.A., 2021. A comparative study of prevalence antimicrobials resistance *Klebsiella pneumoniae* among different pathogenic bacteria isolated from patients with urinary tract infection in Al-Najaf City, Iraq. *Latin American Journal of Pharmacy*, 40(SI), 174-178.

[30] Aljanaby, A.A.J., Al-Faham, Q.M.H., Aljanaby, I.A.J. and Hasan, T.H., 2022. Immunological role of cluster of differentiation 56 and cluster of differentiation 19 in patients infected with mycobacterium tuberculosis in Iraq. *Gene Reports*, 26(3), DOI: 10.1016/j.genrep.2022.101514.

[31] Ke, J., Jin, S., Han, B., Yan, H. and Shen, D., 1997. Hydrogen bonding of some organic acid in supercritical CO2 with polar cosolvents. *The Journal of Supercritical Fluids*, 11(1-2), 53-60.

[32] Waheeb, A.S., Kyhoiesh, H.A.K., Salman, A.W., Al-Adilee, K.J. and Kadhim, M.M., 2022. Metal complexes of a new azo ligand 2-[2'-(5-nitrothiazolyl) azo]-4-methoxyphenol (NTAMP): Synthesis, spectral characterization, and theoretical calculation. *Inorganic Chemistry Communications*, 138, DOI: 10.1016/j.inoche.2022.109267.

[33] Jawad, S.A.A. and Kareem, I.K., 2022. Synthesis, characterization of new azo-Schiff ligand type N_2O_2 and metal complexes with Di valance nickel, palladium and tetra valance platinum. *NeuroQuantology*, 20(1), 62-70.